A Framework for Autonomous Near-Earth Object Precovery

Amelia A. Skeers[1] and Tam N. Nguyen[2]
University of Maryland, College Park, MD, 20740, United States

Near-Earth Objects (NEOs) that are sufficiently large and close enough to Earth pose a risk of disastrous collisions. The detection of these objects represents the critical first step in mitigating potential impact risk. One of the primary methods for identifying moving objects is to link three separate tracklets of detections, which can take up to multiple weeks. With the introduction of powerful observatories like the Vera C. Rubin Observatory and NEO Surveyor, supplementary methods of detection are needed to accommodate the dramatic increase in new detections. Precovery is a detection process that finds an object in archival observatory data to refine its orbit, reducing the need for follow-up observations. Target objects are generally too faint for older observatories to detect, but they can be revealed with image processing. Precovery is currently used on a case-by-case basis but has the potential to become another fast and reliable method for identifying NEOs. This paper presents a proof-of-concept framework for automating precovery through a streamlined software pipeline. The developed Python framework integrates astronomical online tools and software packages. The pipeline starts with an object's initial orbital elements and physical parameters from NASA, propagates backward in time, filters for observable states, and queries archival images with the predicted positions. The system then uses image timestamps and observatory locations to re-propagate the object and achieve more accurate states, which are used to retrieve image data for object detection. The pipeline was validated using three well-characterized NEOs of different Near-Earth orbit classes, and the results were compared with NASA's JPL Horizons ephemeris data. These comparisons showed agreement between the predicted position and the actual position, with offsets below 0.1 arcseconds. This level of precision on constrained objects is a strong benchmark for the framework's performance. The pipeline is also equipped to handle orbit uncertainty through covariance propagation. The current framework delivers the images and predicted locations; future work will incorporate image processing to complete the automation process. This framework for a fully autonomous precovery system reduces the manual nature of current precovery methods. The streamlined precovery process could augment other detection algorithms in confirming the thousands of NEOs that powerful new observatories like Vera C. Rubin will discover. This proof of concept demonstrates the potential for precovery to quickly quantify NEO populations and support planetary defense efforts.

I. Introduction

Near-Earth Objects (NEOs) are defined as asteroids and comets that are less than 1.3 AU from the Sun on their closest approach (perihelion distance) [1]. Potentially Hazardous Asteroids (PHAs) are a subset of NEOs which threaten disastrous collisions due to their size (diameter of 140 meters, corresponding to an absolute magnitude (H) of <22) and distance from Earth (minimum orbit intersection distances (MOID) < 0.05 AU) [2]. In 2005, Congress instructed NASA to discover 90% of NEOs larger than 140 meters by 2020 [3]. This benchmark has not been reached. In fact, less than 50% of these NEOs have been found as of April 2025 [4]. This population of asteroids is especially dangerous because they are large enough to cause significant damage, but often fainter than observatories can find without advanced search methods.

[1] Undergraduate Student, Department of Aerospace Engineering.
[2] Assistant Professor, Department of Aerospace Engineering.

Many surveys have contributed to the growing catalog of detected NEOs. These surveys have been productive, but they are unable to detect every object with H<22. Objects' apparent magnitudes can be fainter than their absolute magnitude, depending on their distance and viewing geometry, and often fall below the limiting magnitude of surveys. The Catalina Sky Survey, for example, has a limiting magnitude of about 21.5 [5]. Multiple new and upcoming missions aim to address the challenge of finding NEOs beyond the detection capabilities of current surveys. NEO Surveyor is a space telescope scheduled to launch in 2027, with the primary mission of documenting 2/3 of all PHAs [6]. Its location will enable it to find NEOs in the direction of the Sun and NEOs with low albedos. The Vera C. Rubin Observatory (Rubin) is projected to detect between 60%-85% of all PHAs with diameters greater than 140 meters [7]. Rubin can accomplish these feats because of its 3.2-gigapixel digital camera [8]. During its 10-year operation, it will be used to study dark matter and dark energy, map the Milky Way, and find asteroids.

There are several methods for NEO detection, and each has limitations. Rubin will employ two primary detection methods. The first is to identify trailed objects, as trails are one characteristic of a sufficiently bright and fast-moving object in a prolonged exposure [9]. The second, and primary, NEO detection method is the Moving Object Processing System (MOPS) which finds groups of two or more detections on the same night, called tracklets, and links them to other tracklets found on separate nights [10]. The first detection method, identifying trailed objects, only works on a small subset of NEOs. The MOPS method works well for detecting NEOs, but it can take two weeks for the required three tracklets to be found. Detections also generally require follow-ups, either from the same observatory that detected the object or from a separate one. Detections are propagated forward and telescopes are directed to look at the new expected location in order to confirm it as an NEO. One problem with this is that telescope time is expensive, and another is that observation arcs of NEOs are often not ideal for long stretches of time. This can mean that an object is discovered, but it may not be observable again for months, by which time the calculated orbit would have propagated with potentially substantial errors.

Precovery of NEOs is an alternative method for constraining the orbits of newly detected objects, without the need for follow-up observations. Instead, it scours past archival image data from surveys like Catalina, ATLAS, and Pan-STARRS. Previous precovery studies found new observations of NEOs on a case-by-case basis, which is not efficient for the large number of detections that will come from Rubin and Surveyor, and can only work for sufficiently bright objects [11, 12]. Target objects (H up to 22) can be too faint for surveys to detect initially, and one solution to address the problem of faint objects is to improve the signal-to-noise ratio of the target with image processing. Image processing to reveal observations of faint and unconstrained objects can be computationally expensive, but new approaches like the fast discrete X-ray transform (FaXT) address this challenge [13]. Combining precovery with modern image processing is an approach that addresses several of the challenges involved in detecting and tracking faint NEOs. Streamlining this precovery system would augment the current methods that tackle the daunting task of confirming the thousands of NEOs Rubin, and later Surveyor, will discover.

This work aims to support planetary defense efforts and is a proof of concept for making precovery autonomous and efficient. The result is a framework for a software pipeline to take an unconfirmed object and find more detections using precovery techniques, extending the object's observation arc. The pipeline integrates existing astronomical pipelines, APIs, and packages in Python and connects them through intermediate filtering, conversion, and calculation steps. This framework is intended to be both a benchmark for precovery's feasibility on a large scale and the first step in building a robust and efficient tool for detecting and characterizing NEOs.

II. Approach

The construction of the Python pipeline first required a high-level vision of the architecture needed to get from object detection to image retrieval. From this framework, existing tools were evaluated for the accomplishment of individual tasks. New components were created to address tasks that existing tools could not. Creating one streamlined pipeline also called for the interfacing of each block, so the inputs and outputs of each component were transformed to accommodate the requirements of the next, often through intermediate calculations and conversions. Continuous validation is another essential piece in program construction, and this was continuously accomplished using known bodies as well as the target unconfirmed bodies. Both subsets required different data handling, and the program's ability to accommodate both was a priority. The primary parts of the pipeline are outlined in Fig. 1 on the next page and discussed in this section.

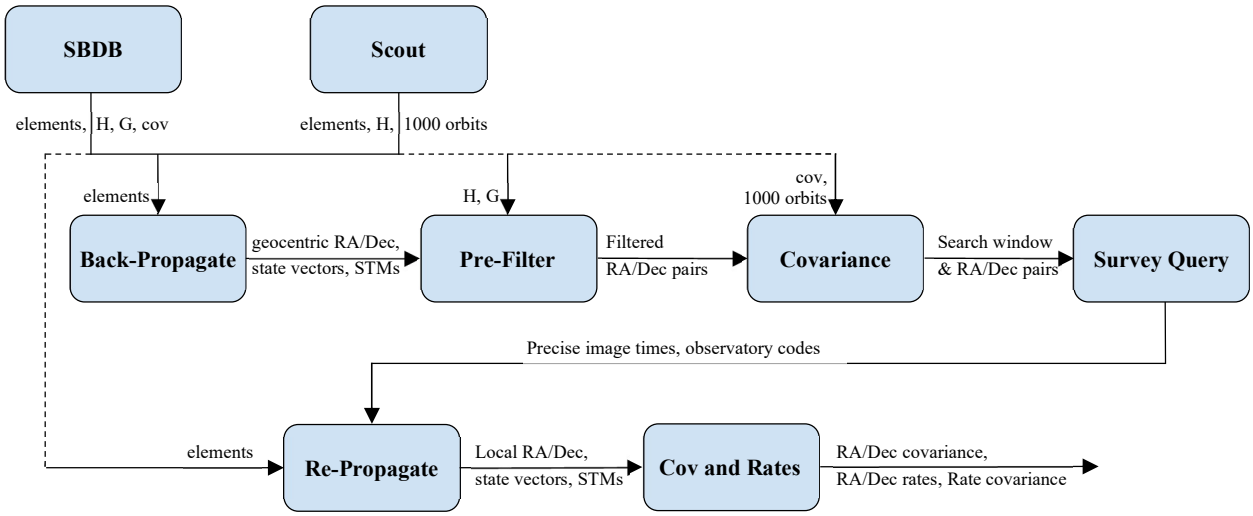

Fig. 1 Automated Precovery Architecture.

A. Object Data Retrieval

The first step in the pipeline is to retrieve data about the target object, which is either a confirmed object from NASA JPL's Small Body Database (SBDB) or an unconfirmed object from the Near-Earth Object Confirmation Page's Scout Database [14, 15]. The confirmed SBDB objects are valuable as validation tests, since it is simple to check for accuracy by comparing the results to the true ephemeris data. The eventual goal, however, is to apply this pipeline on unconfirmed objects, obtained from Scout. SBDB's API is called to retrieve the cometary elements and physical parameters for the specified object. Scout's API provides 1000 potential orbits, which need to be averaged in the pipeline prior to propagation. The cometary elements are used for propagation and the physical parameters, absolute magnitude and slope parameter, are important for determining when an object should be visible from Earth.

B. Back-Propagation

The next step propagates the retrieved orbital elements backward in time with a Python package, the Gauss-Radau Small-body Simulator (GRSS) [16]. This is an initial pass, and therefore geocentric state vectors are collected for the NEO instead of exact observatory-based states. The state vectors from the Sun to the Earth are also retrieved. These state vectors are only needed for the filtering step, which follows propagation. The geocentric right ascension and declination (RA and Dec) are fetched for each propagated time step, and these coordinates are ultimately used for querying astronomical survey images. Figure 2 below shows the orbit for 2024 YR4, which the pipeline propagated in GRSS and plotted using state vectors.

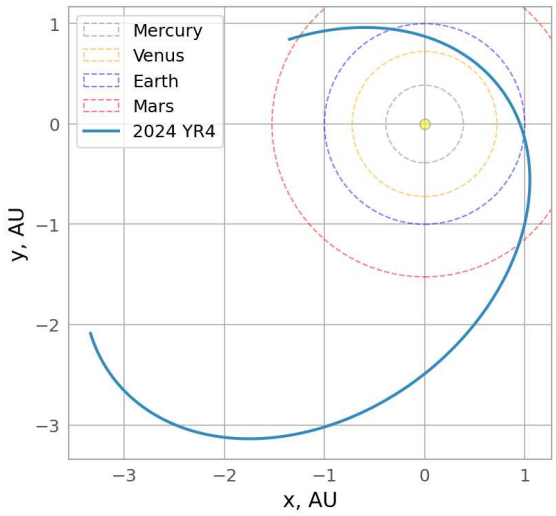

Fig. 2 2024 YR4's orbit propagated back 1000 days from Jan. 30, 2025 in GRSS

C. Pre-Filter

The next step is entirely programmed in Python; it uses the state vectors from the propagation step and the physical properties from the retrieval step to calculate solar elongation, solar phase angle, and visual magnitude of the NEO. These three values quantify potential visibility. Solar elongation is the angle between the Sun and the target as viewed from the Earth and is given by

$$\theta = \arccos\big((-\boldsymbol{R}\cdot\boldsymbol{\rho})/(\|\boldsymbol{R}\|\,\|\boldsymbol{\rho}\|)\big) \tag{1}$$

where **R** is the heliocentric position vector of the Earth and **ρ** is the geocentric position vector of the NEO. Solar elongation less than 60° implies that the object is too close to the Sun to be viewed from Earth. Solar phase angle is the angle at the NEO between the Sun and the Earth and is given by

$$\phi = \arccos\big((\boldsymbol{r}\cdot\boldsymbol{\rho})/(\|\boldsymbol{r}\|\,\|\boldsymbol{\rho}\|)\big) \tag{2}$$

where **r** is the heliocentric position vector of the NEO. A solar phase angle greater than 120° signals that the lit face of the asteroid does not face the Earth. Visual magnitude is a measure of an object's apparent brightness relative to an observer and is calculated with the position vectors, solar phase angle, absolute magnitude, H, and slope parameter, G [17].

$$V = H + 5\log(r\rho) - 2.5\log\big((1-G)\exp(-3.33(\tan(0.5\phi))^{0.63}) + G\exp(-1.87(\tan(0.5\phi))^{1.22})\big) \tag{3}$$

V fainter than 24 is the observability limit set by this project, which is a representative limit for Rubin's bands [8]. Entries that are not likely to be observable based on these three conditions are filtered out.

D. Covariance Calculation

Unconfirmed objects have uncertain orbits, and propagation leads to greater uncertainty. For this reason, covariance is another necessary consideration in the precovery process. It is needed to determine how large a search window needs to be to find an object. SBDB includes initial covariance for known bodies, making covariance propagation simple. However, the unconfirmed objects from Scout do not. Just as the 1000 orbits from Scout were used to calculate a mean orbit, covariance can be calculated. The initial covariance from SBDB and the calculated covariance from Scout are then propagated to the final time step with a state transition matrix. GRSS returns STMs in cometary-to-Cartesian form, so the Jacobian of the initial cometary elements with respect to the initial Cartesian state is also calculated, and the two are multiplied to compose the Cartesian-to-Cartesian STM. GRSS also provides the observation Jacobian, and so the covariance propagation is

$$P_\theta = H\,\Phi\,P_0\,\Phi^T\,H^T \tag{4}$$

Where P_θ is the final covariance in RA/Dec space, P_0 is the initial covariance in Cartesian space, H is the observation Jacobian, and Φ is the Cartesian-to-Cartesian STM. The search window limit is set by the 3-sigma radius calculated from the covariance, which ensures that the survey query looks everywhere that the object might be but does not use a search window that is unnecessarily wide.

E. Survey Query

The entries remaining after the filter step are fed to the next integrated API. The Comet-Asteroid Telescopic Catalog Hub (CATCH) is an API created by the Small Bodies Node of the NASA Planetary Data System group at the University of Maryland, which retrieves archival image data from several astronomical surveys [18]. The software pipeline queries CATCH with each time and RA/Dec pair, as well as the search window limit in arcminutes, and collects the data for each image that is returned from the queries.

F. Re-propagation

The precise time and source observatory of each of the images are then fed back into GRSS for propagation. The RA and Dec are collected from the exact image times, relative to the respective observatory's location, instead of geocentric like the first pass. This refines the expected location of the targeted object in each image.

G. Covariance and Rates Calculation

The downstream image processing requires more than just the resulting position and times for accuracy. Once again, RA/Dec covariance is calculated after the propagation step. However, instead of only propagating covariance to the last time step, it is calculated at each time step, which still follows the form shown in Eq. (4). The direction of uncertainty conveys the direction of motion of the object, since error more often accumulates in the along-track direction than the cross-track. Image processing further necessitates knowing the RA and Dec rates of the object, which are calculated and stored at each time, as

$$dRA/dt = \left(xv_y - yv_x\right)/(x^2 + y^2) \tag{5}$$

$$dDec/dt = -(x^2 + y^2)^{-1/2}\left(v_z - z/r^2\left(xv_x + yv_y + zv_z\right)\right) \tag{6}$$

where $\mathbf{r} = (x, y, z)$ is the position vector from the observatory to the object and $\mathbf{v} = (v_x, v_y, v_z)$ is the velocity vector. The covariances of the rates are also calculated, similarly to Eq. (4). The final calculation is estimated visual magnitude, as previously shown in Eq. (3), which allows for an additional observability filter during image processing.

H. Validation

The above steps are the major components of the envisioned pipeline, but extensive validation is necessary between the second propagation and image processing steps. The goal for this pipeline is to constrain the orbits of unconfirmed objects, and their orbital data will include uncertainty. Therefore, the pipeline must be as precise as possible, to reduce the propagated uncertainty. Known NEOs from SBDB allow for comparison with JPL ephemeris data to ensure accuracy down to less than an arcsecond. CATCH has a moving body query which uses JPL data to return exact object positions and running that with a known body allows comparison with the pipeline, ensuring the same images and coordinates are returned in both queries.

III. Results

The pipeline is completed through the re-propagation and following calculations steps. The pipeline also has the capability to download the archival images (FITS format) and display them for analysis.

A. Confirmed NEO Validation

As mentioned above, a large portion of this work was to validate the framework on known NEOs, retrieved from SBDB. One test case is the Apollo-type asteroid Torifune (98943), which crosses Earth's orbit. Running the pipeline for Torifune yields separations of less than a tenth of an arcsecond between the pipeline's prediction and NASA's result, displayed in Fig. 3a. A full run-through of the pipeline also printed FITS images that clearly mark a bright spot, Torifune, moving across the sky. Torifune has a visual magnitude of 17.77 in the FITS image in Fig. 3b, and an absolute magnitude of 18.71, which means Torifune is often resolvable by multiple surveys.

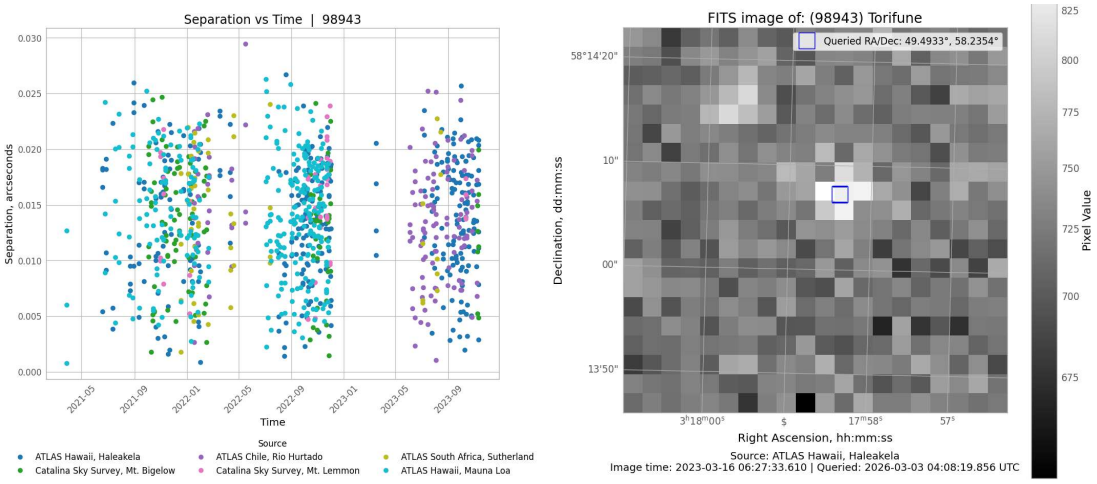

a) Torifune NASA/Pipeline separation scatterplot. **b) FITS image of Torifune on Mar. 16, 2023.**

Fig. 3 Torifune separation plot and FITS image.

Another test object was the Amor-type asteroid Eric (4954), which does not cross Earth's orbit and is much brighter than Torifune, with an absolute magnitude of 12.56. The three photos below are FITS images resulting from running the pipeline from start to finish with Eric (see Fig. 4). The yellow box is the pipeline's propagated RA/Dec for Eric at these times, and it is centered directly over Eric in the pictures (the separation from NASA data is again less than a tenth of an arcsecond at 0.017 arcseconds), demonstrating another successful validation test for a known body. The objects this pipeline is being designed for will not be as bright as Eric or Torifune, and therefore not as visible in the survey images. It is still valuable to see the pipeline mark an object correctly.

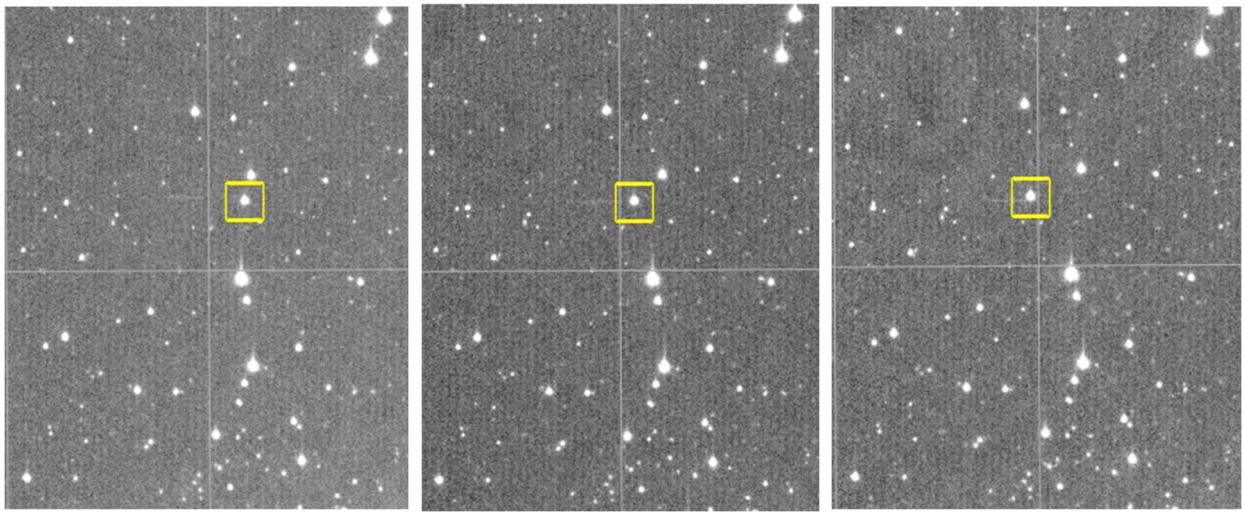

Fig. 4 FITS images of Eric on March 8th, 2014. Yellow boxes are the pipeline's propagated locations for Eric.

The Didymos system (65803) was another primary NEO used for early development, and the results were generally close to the expected results. However, there was a significant jump in RA/Dec separation between the pipeline's propagated locations and NASA's, beginning in September 2022. Figure 5a shows a low-resolution JPG retrieved from CATCH, with the yellow arrow pointing at Didymos, which has a debris trail. Figure 5b is an astronomical FITS image queried from CATCH. The green box marked 'NASA' shows where Didymos is based on ephemeris data, and the yellow marks where the pipeline calculated Didymos to be. The trailed object and NASA's position match, but the pipeline's position is offset by nearly an arcminute.

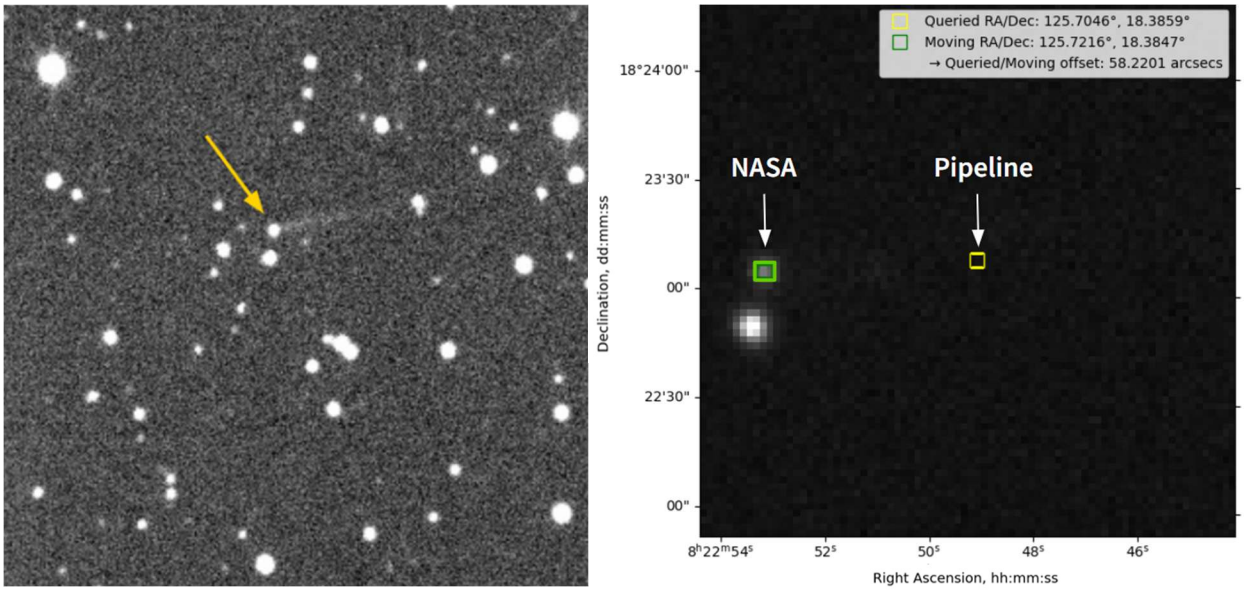

a) Didymos system with debris trail. **b) Didymos predicted locations on Nov. 25, 2022.**

Fig. 5 Didymos images returned from CATCH query.

Figure 6 is a scatterplot of the separation between NASA's and the pipeline's predicted RA and Dec, which has a peak of nearly 300 arcseconds in Fall 2022. The Double Asteroid Redirection Test (DART) impacted Didymos' moon Dimorphos on September 26, 2022, which is the cause of the trail in Fig. 5a [19]. The Fall 2022 jump revealed some inaccuracies in the pipeline, which exposed its extreme sensitivity, not to DART's impact, but to Didymos' close approach to Earth (<0.1 AU) [19].

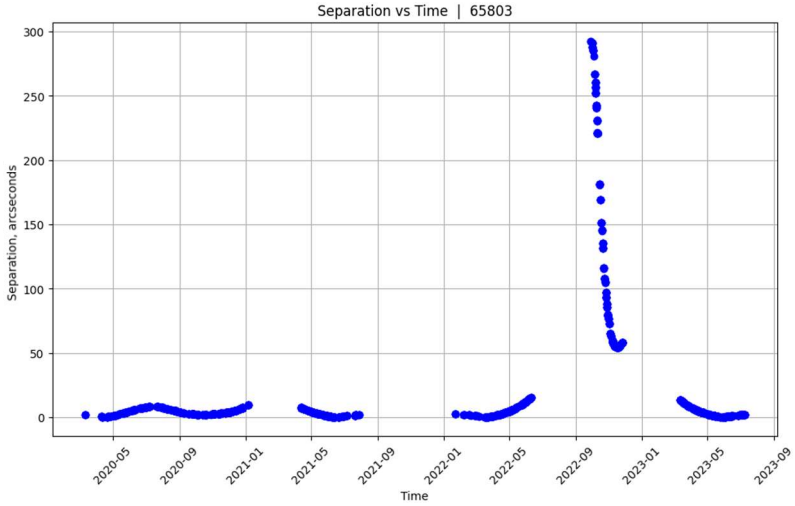

Fig. 6 Separation between NASA's propagated location for Didymos system and the pipeline's.

The validation results also originally demonstrated jumps in separation when Torifune crossed Earth's orbit directly in front or behind Earth, suggesting that accuracy went down the closer an object gets to Earth. These problems were resolved through more careful planning of the propagation time conversions between TDB and UTC, as well as accurate locations of the various observatories used to collect images. Prior to this, the pipeline was still using geocentric positions for image collection, which is fairly accurate when objects are further from Earth. However, as objects get close to Earth, knowing the precise location of the telescopes taking pictures is essential.

After these improvements, the pipeline was tested with the Didymos system again. The results no longer jump after the DART impact, and the separation from NASA data is less than a tenth of an arcsecond, as seen in the Fig. 7a scatterplot below. This confirms that the pipeline is not only accurate, but also no longer sensitive to anomalies like close encounters with Earth and planetary defense impact missions. The FITS image in Fig. 7b is from November 2022, two months after Didymos' close approach and the DART mission. The blue box hovering directly in the middle of the white spot shows that the pipeline accurately predicted Didymos' location, with an offset from NASA's location, marked by the smaller green box, of 0.02 arcseconds.

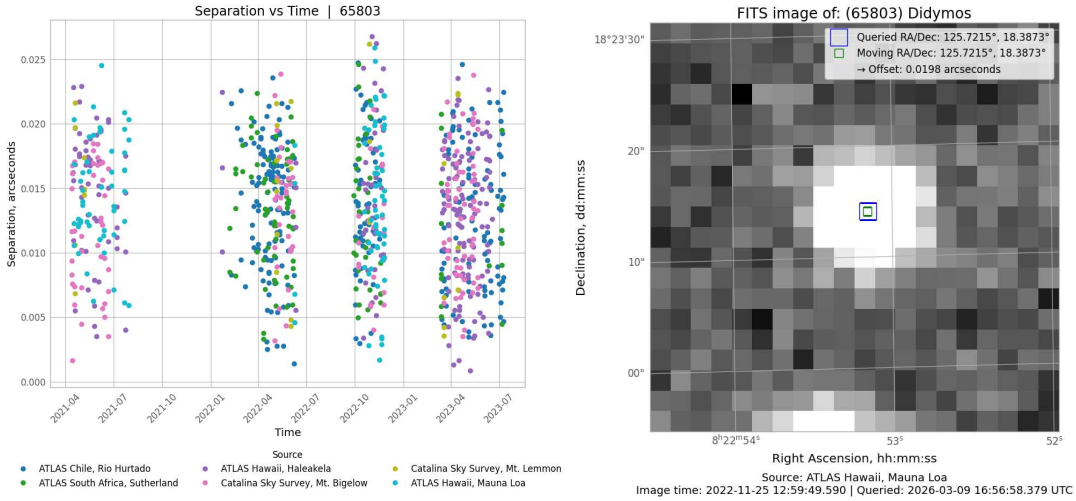

a) Didymos NASA/Pipeline separation scatterplot. **b) Didymos predicted locations on Nov. 25, 2022.**

Fig. 7 Didymos separation plot and FITS image after pipeline position correction.

B. Unconfirmed NEO Validation

After demonstrating the accuracy of the pipeline with known objects, focus shifted to unconfirmed objects in Scout. The 1000 orbits provided by Scout were used to get the mean orbit and initial covariance matrix, which were then propagated and plotted to determine the uncertainty of the object's position at the final time. The 3-sigma uncertainty ellipse from the propagated covariance gives CATCH its search radius, in arcminutes. The accuracy of the covariance propagation was validated by propagating all 1000 of the orbits Scout provides to the same epoch, and plotting them with the 1-, 2-, and 3-sigma ellipses from the covariance. The test is valid if most of the Scout orbits are within the 1-sigma ellipse, then more in the 2-sigma ellipse, and almost none outside of the 3-sigma ellipse.

The Scout object P22cviJ has low uncertainty and is therefore a good validation case. Figure 8a shows its mean orbit and 1000 sampled orbits propagated 2000 days into the past, and the 1-, 2-, and 3-sigma covariance ellipses which contain approximately 39%, 86%, and 99% of the orbits, respectively. Due to the object's low uncertainty, the ellipses are very narrow and elongated, with a maximum 3-sigma radius of 0.00364 degrees, or 0.2184 arcminutes. Some Scout objects will have more uncertainty than P22cviJ, with maximum radii over the CATCH limit of 120 arcminutes. However, for Scout objects with more defined orbits, covariance is a valuable tool for reducing the search query load on CATCH and the subsequent image processing steps. Figure 8b is an illustration of another Scout object's covariance. The pipeline propagated object C17GY55 for 500 days, a fourth of the time as for P22cviJ. It better shows the ellipses and the concentration of points within them.

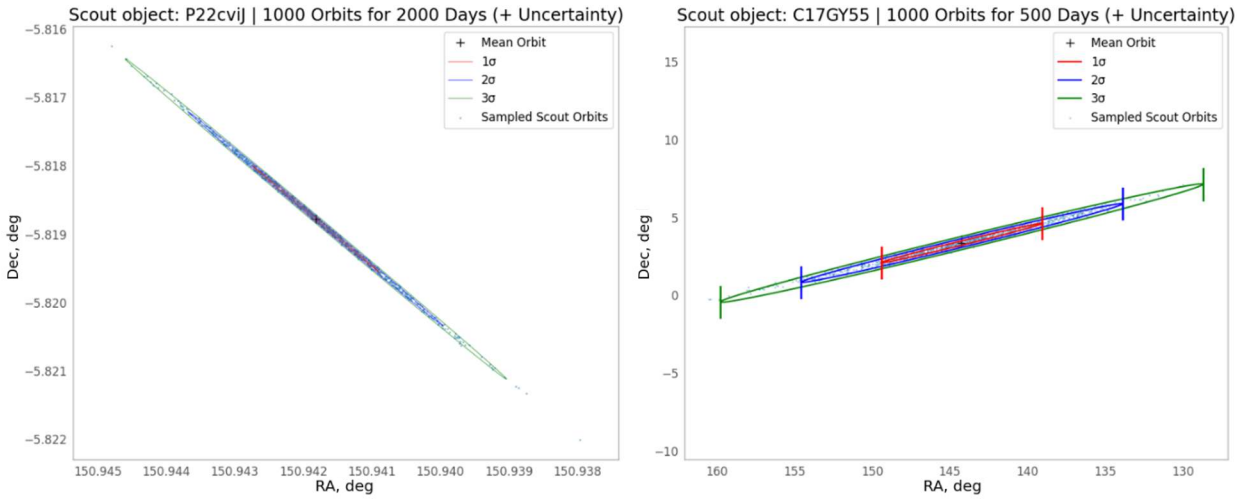

a) P22cviJ back-propagated 2000 days. **b) C17GY55 back-propagated 500 days.**

Fig. 8 Scout objects' mean orbit, covariance ellipses, and 1000 sample orbits after back-propagation.

The validation tests of these two Scout objects and others confirm that the covariance propagation matches the propagation of the initial 1000 orbits. Now the pipeline no longer needs to propagate 1000 orbits since the covariance captures the same information with far less computation and time. Covariance dictates the span of images that the object could be found in, while also providing information about how the object is moving. These two aspects together allow for image stacking to be accomplished as efficiently and accurately as possible.

The successful validation of the different parts of the pipeline demonstrates that the Python pipeline flows from step to step seamlessly and accurately. Image processing, orbit constraining, and impact analysis will follow to finish the full pipeline.

IV. Conclusion

This work presents a milestone on the path to autonomous precovery. The approach builds on previous astronomical techniques and tools, and it adds components unique to the method of precovery. The pipeline begins with an initial orbit for an object, which it propagates to the past and determines when and where it may have been visible to surveys that could not see it before. It uses the data from these images to re-propagate the object to the time the images were taken, documenting its coordinates, rates of motion, and errors. The pipeline ends with providing the object's orbital data and images from the surveys where the object could be found. The outputs of the pipeline enable further progress on an autonomous method for uncovering detections of new NEOs and constraining their orbits using archival images. The validation results of this study demonstrated the pipeline's accuracy, as propagated data matched

NASA's data for confirmed objects, and Scout covariance data matched the brute force propagation data of all 1000 provided orbits.

The process also included experimentation when deciding which existing tools to use, which components to build, and how best to package data for the steps that follow the pipeline. The puzzle of orbital elements conversions, time scales, telescope data, and various calculations began with an extended number of packages addressing each sub-step of a component. Streamlining the pipeline required reducing the use of external tools where possible and developing internal pieces that are efficient and well-structured to allow for future researchers to build on it seamlessly. The result is the approach outlined in this paper, which in turn produced validation results that indicate its readiness to be a foundational piece of more precovery steps to come.

Future work on this precovery framework includes image processing to uncover the faint observations and fitting the new observations to the existing orbit, confirming the object as legitimate. Dr. Tam Nguyen and the Strategic Space Sensing Lab at UMD are working on these steps. Dr. Nguyen has previously done image processing for a similar task, to uncover observations in data from the Transiting Exoplanets Survey Satellite (TESS) [13]. Orbit determination features will follow after detections are uncovered, after which the confirmed orbits will be submitted to the Minor Planet Center (MPC). Additionally, a team in the Space Exploration Sector at the Johns Hopkins University Applied Physics Lab is developing object characterization features, to include impact probability and risk assessment of the objects that the pipeline uncovers.

The primary objective of this project was to prove that precovery could be an efficient way of improving the orbits of new NEOs. The current framework and results are promising and demonstrate that this method could reliably assist innovative technologies and missions like the Rubin Observatory with NEO discovery and characterization. NASA's Planetary Defense Coordination Office (PDCO) set forth focus areas for protecting against devastating impacts [14]. This project focused on the first: Search, Detect, and Track. Current and future work will be built on this framework to further address that pillar. Automated image processing will reveal new detections, and the new detections will be used to fit the uncertain objects. Combined with the methods used by other asteroid tracking teams, this research is poised to enhance capabilities to quantify NEO populations, assess collision risks, and support future planetary defense efforts.

Acknowledgments

This research project was conducted through the Aerospace Engineering Honors Program at the University of Maryland and within the Strategic Space Sensing Laboratory. The authors acknowledge support from the ASTRA–UMD / Johns Hopkins University Applied Physics Laboratory Joint Summer Internship in Spacecraft Engineering, which provided funding and mentorship for this work. The authors thank Dr. Justin Atchison and Dr. Rylie Bull of the Johns Hopkins University Applied Physics Laboratory for their guidance in the development and execution of this project. The authors also thank Dr. Rahil Makadia, developer of the GRSS software package, for accommodating feature requests that supported this work. The authors thank Dr. Alison Flatau for connecting the student author with the research advisor at the beginning of this project.

References

[1] Morbidelli, A., Bottke, W. F., Jr., Froeschlé, Ch., and Michel, P., "Origin and Evolution of Near-Earth Objects," *Asteroids III*, edited by W. F. Bottke, Jr., A. Cellino, P. Paolicchi, and R. P. Binzel, University of Arizona Press, Tucson, 2002, pp. 409–422.

[2] Ivezić, Ž., Tyson, J. A., Jurić, M., Kubica, J., Connolly, A., Pierfederici, F., Harris, A. W., Bowell, E., and the LSST Collaboration, "LSST: Comprehensive NEO Detection, Characterization, and Orbits," *Proceedings of the International Astronomical Union*, Vol. 2, No. S236, 2006, pp. 353–362.
doi: 10.1017/S1743921307003420

[3] U.S. House of Representatives, "George E. Brown, Jr. Near-Earth Object Survey Act," H. Rept. 109-158, June 2005.

[4] NASA Office of Inspector General, "NASA's Implementation and Management of Its Planetary Defense Strategy," Report No. IG-25-006, NASA, Washington, DC, June 2025.

[5] Christensen, E., Larson, S., Boattini, A., Gibbs, A., Grauer, A., Hill, R., Johnson, J., Kowalski, R., and McNaught, R., "The Catalina Sky Survey: Current and Future Work," *AAS/Division for Planetary Sciences Meeting Abstracts*, Vol. 44, American Astronomical Society, 2012, Abstract 210.13.

[6] Mainzer, A. K., et al., "The Near-Earth Object Surveyor Mission," *The Planetary Science Journal*, Vol. 4, No. 12, 2023, p. 224.
doi: 10.3847/PSJ/ad0468

[7] Chesley, S. R., and Vereš, P., "Projected Near-Earth Object Discovery Performance of the Large Synoptic Survey Telescope," JPL-Publ-16-11, NASA Jet Propulsion Laboratory, Apr. 2017.

[8] LSST Science Collaborations and LSST Project, "LSST System Design," *LSST Science Book,* Version 2.0, LSST Corporation, Tucson, 2009, pp. 25–52.

[9] Jones, R. L., Slater, C. T., Moeyens, J., Allen, L., Axelrod, T., Cook, K., Ivezić, Ž., Jurić, M., Myers, J., and Petry, C. E., "The

Large Synoptic Survey Telescope as a Near-Earth Object Discovery Machine," *Icarus*, Vol. 303, 2018, pp. 181–202. doi: 10.1016/j.icarus.2017.11.033
[10] Denneau, L., et al., "The Pan-STARRS Moving Object Processing System," *Publications of the Astronomical Society of the Pacific*, Vol. 125, No. 926, 2013, p. 357. doi: 10.1086/670337
[11] Gwyn, S. D. J., Hill, N., and Kavelaars, J. J., "SSOS: A Moving-Object Image Search Tool for Asteroid Precovery," *Publications of the Astronomical Society of the Pacific*, Vol. 124, No. 916, 2012, p. 579. doi: 10.1086/666462
[12] Naidu, S. P., Micheli, M., Farnocchia, D., Roa, J., Fedorets, G., Christensen, E., and Weryk, R., "Precovery Observations Confirm the Capture Time of Asteroid 2020 CD3 as Earth's Minimoon," *The Astrophysical Journal Letters*, Vol. 913, No. 1, 2021, p. L6. doi: 10.3847/2041-8213/abf836
[13] Nguyen, T., Woods, D. F., Ruprecht, J., and Birge, J., "Efficient Search and Detection of Faint Moving Objects in Image Data," *The Astronomical Journal*, Vol. 167, No. 3, 2024, p. 113. doi: 10.3847/1538-3881/ad20e0
[14] NASA Jet Propulsion Laboratory, "SBDB API," https://ssd-api.jpl.nasa.gov/doc/sbdb.html [retrieved 20 November 2025].
[15] NASA Jet Propulsion Laboratory, "Scout API," https://ssd-api.jpl.nasa.gov/doc/scout.html [retrieved 20 November 2025].
[16] Makadia, R., Farnocchia, D., Chesley, S. R., and Eggl, S., "Gauss-Radau Small-Body Simulator (GRSS): An Open-Source Library for Planetary Defense," *The Planetary Science Journal*, Vol. 6, No. 4, 2025, p. 85. doi: 10.3847/PSJ/adbc88
[17] Bowell, E., Hapke, B., Domingue, D., Lumme, K., Peltoniemi, J., and Harris, A. W., "Application of Photometric Models to Asteroids.," *Asteroids II*, edited by R. P. Binzel, T. Gehrels, and M. S. Matthews, University of Arizona Press, Tucson, 1989, pp. 524–556.
[18] NASA Planetary Data System Small Bodies Node, "CATCH," https://catch.astro.umd.edu/apis [retrieved 21 August 2025].
[19] Adams, E., Chabot, N., Cheng, A., Rivkin, A., Reynolds, E., and Shearer, C., "Double Asteroid Redirection Test (DART) Mission," APL_COMM-23-04772, Johns Hopkins University Applied Physics Laboratory, Laurel, MD, Oct. 2023.